



## PREPARATION OF ZEOLITIC MATERIAL USING NATURAL CLINOPTILOLITE FOR CO<sub>2</sub> CAPTURE

### PREPARACIÓN DE UN MATERIAL ZEOLÍTICO UTILIZANDO CLINOPTILOLITA NATURAL PARA LA CAPTURA DE CO<sub>2</sub>

A. Sánchez-Ruíz, I. Robles-Gutiérrez, F. Espejel-Ayala\*

Centro de Investigación y Desarrollo Tecnológico en Electroquímica. Parque Industrial Querétaro, Sanfandila s/n, Pedro Escobedo 76703, Querétaro, México.

Received January 24, 2018; Accepted February 13, 2018

#### Abstract

This study shows the results in the preparation of zeolite P using a natural clinoptilolite. Three samples of clinoptilolite were analyzed to determine the sample with high purity of clinoptilolite; however, quartz and albite also were identified in the samples. The synthesis of zeolitic material was achieved in a hydrothermal system considering five factors: dose of CTAB, temperature, time of reaction, solid/liquid ratio and NaOH concentration. A factorial experimental design was implemented and 32 experiments were achieved. The obtained samples were characterized by XRD, SEM and N<sub>2</sub> physical adsorption. The principal factor in the formation of zeolite P was the concentration of NaOH. The zeolite P synthesized was impregnated with diethanolamine (DEA) and used to capture CO<sub>2</sub> obtained a value of 2.5 mmol/g as CO<sub>2</sub> adsorption capacity.

**Keywords:** clinoptilolite, CO<sub>2</sub> capture, amine, zeolite P, hydrothermal synthesis.

#### Resumen

Este estudio muestra los resultados de la preparación de zeolita P utilizando una zeolita natural clinoptilolita. Tres muestras de clinoptilolita fueron analizadas para determinar la muestra de mayor pureza; se identificó clinoptilolita, además de cuarzo y albita en las tres muestras. La síntesis del material zeolítico se realizó en un sistema hidrotermal que consideró cinco factores: dosis de CTAB, temperatura y tiempo de reacción, relación sólido/líquido y concentración de NaOH. Se implementó un diseño factorial de 32 experimentos. Las muestras obtenidas fueron caracterizadas mediante XRD, MEB y adsorción física de nitrógeno. Los principales factores involucrados en la formación de la zeolita P fue la concentración de NaOH. La zeolita P sintetizada fue impregnada con dietanolamina y utilizada en la captura de CO<sub>2</sub> con la cual se obtuvo una capacidad de adsorción de hasta 2.5 mmol/g.

**Palabras clave:** clinoptilolita, captura de CO<sub>2</sub>, aminas, zeolita P, síntesis hidrotermal.

## 1 Introduction

There are three principal processes to capture CO<sub>2</sub> (CC) from atmosphere: absorption, adsorption and separation by membranes. Absorption use liquid solutions of amines; methylamine (MEA) is the most used amine (Yang *et al.*, 2008) for its high selectivity to acid gases. For example, the process Econamine FG Plus (30 %wt. aqueous MEA solution) can capture 330 tonnes CO<sub>2</sub>/day (Steenveeldt *et al.*, 2006). In spite of high efficiencies, the energy used to regenerate the amines represents 70% of the costs in the CC systems. Moreover, amines are degraded when they are regenerated by heating. The use of membranes is a technology in development that promises relevant

results. Inorganic membranes are the most studied for their high-temperature application. Membranes made from alumina, carbon, glass, silicon carbide, titania, zeolites, and zirconia, supported on different substrates, such as  $\alpha$ -alumina,  $\gamma$ -alumina, zirconia, other zeolites or porous stainless steel (Yang *et al.*, 2008).

Zeolites are used in many fields like wastewater treatment, gases separation and catalysis because their acid and basic properties and geometrical selectivity, principally. In gas separation, zeolites have been used for gases purification by adsorption or geometrical selectivity. Several zeolites have been evaluated at low temperatures, <100° C, and medium-high pressures (100-800KPa) to CC. The Table 1 shows some reported studies for the CC with zeolites.

\* Corresponding author. E-mail: fespejel@cideteq.mx  
doi: 10.24275/10.24275/uam/izt/dcbi/revmexingquim/2018v17n2/Sanchez  
issn-e: 2395-8472

Table 1. Adsorption capacity of CO<sub>2</sub> of zeolites.

Zeolite (pore size, nm)	(Temperature/Pressure/Technique)	Adsorption capacity (mmol/g)	Reference
ZSM-5 (nr)	0-100°C/nr /TGA	2.6	Lee <i>et al.</i> (2015)
Zeolite 13X (0.24)	0-75°C/400-800 KPa/TGA	6	Liu <i>et al.</i> (2014)
Zeolite 5A (0.20)		5	
Zeolite NaA (nr)	25°C/101 KPa /TGA	3.7	Kacem <i>et al.</i> (2015)
Zeolite Rho (0.36)	25-800°C/101 KPa/ TGA	3.4	Cheung <i>et al.</i> (2013)
Chabazite (0.37)	0 °C/103 KPa/ Isothermal	5.6	Araki <i>et al.</i> (2012)
Zeolite T (0.36x0.51)	15-40 °C/100 KPa/ Isothermal	4.01	Ridha and Webley, (2009)
Zeolite Y (1.2)	0-25°C/0-101 KPa/ Isothermal	6.45	Jiang <i>et al.</i> , (2013)

nr: not reported

Table 2. Adsorption capacity of CO<sub>2</sub> using mesoporous materials.

Material (pore size, nm)	Temperature/Pressure/Technique	Adsorption capacity (mmol/g)	Reference
MCM-41 (5)	45°C/101 KPa/ Isotherma	2.36	Hefti <i>et al.</i> (2015)
SBA-15 (6.6)	30-75°C/ 1-100 KPa/ TGA	0.5	Sanz <i>et al.</i> (2015)
Silice	120°C/ 101 KPa/ TGA	2.36	Jing <i>et al.</i> (2014)
MCM-41 (3)	25°C/ 101 KPa/ TGA	2.54	Kilntong <i>et al.</i> (2014)
SBA-15 (6.5)		2.66	
MCM-41 (10.9)		6.98	
MCM-41 (9.6)	25-70°C/ 101 KPa/ TGA	5	Lin and Bai, (2012)
MCM-41(8.2)		3.6	
MCM-41 (11.4)	25-100°C/ 101 KPa/ TGA	4.68	Serna-Guerrero and Sayari, (2010)

The adsorption capacities of zeolites superior to 4 mmol/g has been obtained at elevated pressures or low temperature. The average value is about 2.35 mmol/g. Because the CO<sub>2</sub> molecule has a kinetic diameter close to 0.33 nm the diffusion in the pores of zeolites is difficult and the materials with superior pore size for the CC are preferable. Siliceous mesoporous materials have superior preference by adsorption of big molecules due to their great pore size and they also have been used in CC. Table 2 shows some studies of CC with mesoporous materials.

It is important to note a major adsorption capacity of the MCM-41 type material because the average value is about 3.53 mmol/g. This value is approximately 40% more than in the case of zeolites evaluated at the same conditions of temperature and pressure.

For the case of natural zeolites, clinoptilolite is the more abundant worldwide used in wastewater, principally (Pérez-Escobedo *et al.*, 2016). Clinoptilolite can be used too as source of Si and Al. In fact, clinoptilolite have been used in the preparation of traditional ceramic materials (Heydari *et al.*, 2011; San *et al.*, 2003; Hosseini *et al.*, 2015) and the elaboration of cement (Brundu and Cerri, 2015).

In the synthesis of zeolites using clinoptilolite, Kang *et al.*, (1998) achieved the preparation of zeolite P and hidroxysodalite. Joshi and Joshi (1985) synthesized analcime and faujasite type zeolite with

calcic clinoptilolite. de Fazio *et al.*, (2008) studied the hydrothermal transformation of clinoptilolite obtaining zeolite P. Kamali *et al.*, (2009) and Kazemian *et al.*, (2009) synthesized zeolite NaA with clinoptilolite and aluminum sulphate and sodium aluminate. Wang and Lin, (2009) achieved the synthesis of zeolite P, zeolite Y and analcime. Behin *et al.*, (2016) used synthetic clinoptilolite for the synthesis of zeolite P. With the objective of synthesize a mesoporous material, Shindo *et al.*, (2008, 2010) used clinoptilolite and CTAB. The authors demonstrated the formation of MCM-41 type material as well as zeolite P with 3.5 M NaOH solution at 100° C during 72 hours of synthesis.

Zeolite P is a Gismondine type zeolite with Na+ cation of compensation in the extra-framework of zeolite, and a pore size of 0.31x0.45 and 0.28x0.48 nm (Espejel-Ayala *et al.*, 2015). Although these authors achieved an interesting work, the possibility to use the synthesized material to CC was not proposed; moreover, the optimization of parameters of synthesis of zeolites was not achieved. In the present work, the preparation of a zeolitic material is achieved using a Mexican natural zeolite, with quartz and feldspar as principal impurities, in hydrothermal conditions. It is important to note that for natural clinoptilolite the adsorption capacity of CO<sub>2</sub> is low, approximately 0.105 mmol/g (Hernández-Huesca and Aguilar-Armenta, 2002).

## 2 Experimental

### 2.1 Materials

Three natural samples of zeolites were studied from three different regions of Mexico: San Luis Potosi, Puebla and Morelos, identified as Cli1, Cli2 and Cli3, respectively. CTAB surfactant from Aldrich was used as template. NaOH analytical grade mark Aldrich was used for the hydrothermal synthesis. For the functionalization of zeolitic materials diethanolamine (DEA) was used.

### 2.2 Characterization of samples of clinoptilolite

XRD analysis were achieved in a Bruker D8 Advance in a step size of 0.02 from 5-60  $2\theta$ . The chemical composition was implemented by Scanning Electron Microscope coupled with Energy Dispersive X-ray (SEM-EDX) in a Jeol 6510LV equipment.

### 2.3 Preparation of zeolitic material

The preparation of zeolitic material was achieved in a hydrothermal system with NaOH solution. The clinoptilolite sample was chosen considering the sample with high purity of clinoptilolite. A  $2^k$  full factorial design was implemented with  $k=5$ : amount of CTAB, time, temperature, NaOH concentration and solid/liquid ratio. The experimental matrix is showed in the Table 3. Only one replica of the experiments was achieved.

The preparation of zeolitic material was achieved following the modified procedure of Beck *et al.* (1992). In each experiment NaOH solution was placed in a flask; furthermore, CTAB was placed in agitation during 30 minutes. The clinoptilolite was aggregated and the system was placed in reflux at the conditions established in each experiment.

Table 3. Experimental matrix of the  $2^k$  factorial design in the preparation of zeolitic material with natural clinoptilolite.

Variables	Level 1	Level 2
CTAB (g/mL)	0.015	0.03
Time (h)	24	48
Temperature ( $^{\circ}$ C)	60	90
NaOH (M)	1	2
solid/liquid ratio (g/mL)	0.1	0.2

After that, the solid was separated by filtration and rinsed with water ( $80^{\circ}$  C). The sample obtained was dried at  $120^{\circ}$  C during 24 h and finally calcined at  $550^{\circ}$  C during 4 h.

### 2.4 Characterization of zeolitic material

XRD and SEM analysis were achieved in the same conditions described in the characterization of the sample of clinoptilolite. Surface area was carried out in a  $N_2$  adsorption equipment Belsorp mini. The samples were degasified during 24 h at  $200^{\circ}$  C in a flux of  $N_2$ .

### 2.5 Preparation of amino-functionalized zeolitic material

The preparation was followed in accord of Yang *et al.*, (2015) to obtain 10% of DEA in the zeolitic material. DEA was placed in 10 mL of ethanol for 10 minutes. 0.5 g of zeolitic material was placed during 30 min; furthermore, the system was placed at reflux at  $80^{\circ}$  C for 2 hours. Subsequent, the solid was dried at  $50^{\circ}$  C during 12 hours.

### 2.6 $CO_2$ capture tests

Sorption tests were achieved by the adsorption/desorption technique as follow, 200 mg of sample were placed in a glass tube of 9 mm of inner diameter at  $75^{\circ}$  C for 15 min in a flux of 60 mL/min of  $N_2$  and a pressure of 1 atm. Furthermore, flux of  $CO_2$  was implemented at the same temperature and flux. The desorption was monitored until  $110^{\circ}$  C.  $CO_2$  5% in Ar was used.

## 3 Results and discussion

### 3.1 Natural zeolite clinoptilolite characterization

EDX-SEM analysis shows the chemical composition of zeolites (Table 4). The Si/Al ratio values are accord with the typical interval of the natural clinoptilolite. It is important to consider the mineralogical composition because the total Si and Al not belong to the clinoptilolite. Quartz and feldspar are in the samples and affecting the Si/Al ratio. The  $[Al/(Na+K+(Ca/2)+(Mg/2))]$  ratio is a parameter to estimate the possible minerals in the samples.

Table 4. Chemical composition of clinoptilolite samples.

Element	Sample		
	Cli1	Cli2	Cli3
O	47.02	49.98	50.57
Si	37.66	35.47	20.38
Al	8.18	5.65	10.62
Ca	3	2.47	5.67
K	2.14	3.4	3.31
Na	0.66	1.39	3.28
Mg	0.54	0.83	5.58
Fe	0.76	0.78	0.56
Si/Al ratio	4.42	6.04	3.46
$\left[ \frac{Al}{Na+K+Ca/2+Mg/2} \right]$ ratio	0.8	1.23	0.59

Table 5. Mineralogical composition identification in the clinoptilolite samples.

Sample	Composition (XRD)
Cli1	Clinoptilolite, 81.84%
	Quartz, 23.42%
	Albite, 24.74%
Cli2	Clinoptilolite, 36.72%
	Quartz, 24.54%
	Albite, 38.74%
Cli3	Clinoptilolite, 30.05%
	Quartz, 33.80%
	Anorthite, 35.66%

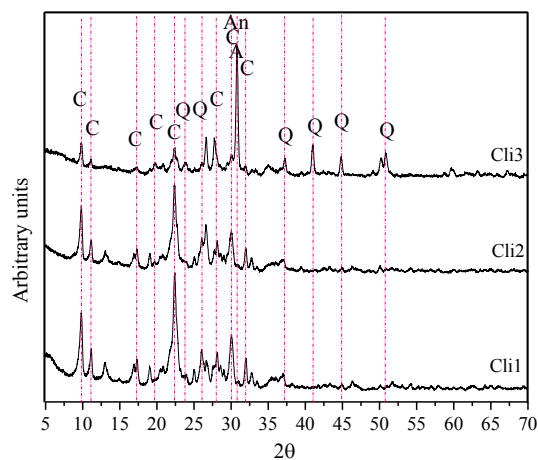


Fig. 1. XRD of clinoptilolite. C: clinoptilolite, Q: quartz; A: albite; An: anorthite.

In the case of zeolites, this value is close to 1; however, for Cli3 the value is 0.53 indicating the presence of feldspar or calcium carbonate. Cli1 and Cli2 have a value close to 1 that is an evidence of high abundance of zeolite clinoptilolite.

The mineralogical composition was identified by XRD and quantified applying the Rietveld method (Table 5). Clinoptilolite is present in 52.8, 36.8 and 30.6% for Cli1, Cli2 and Cli3, respectively. Quartz, albite and anorthite were also identified, as well as, XRD peaks of anorthite were observed in the sample Cli3 (Figure 1).

### 3.2 Results of the synthesis of zeolitic material from natural clinoptilolite

Table 6 shows the mineralogical phases and adsorption capacity of the prepared materials with the natural clinoptilolite by the  $2^k$  design. Zeolite type P was identified in all of the prepared samples; in 12 experiments only was identified zeolite type P. This zeolite has a Si/Al ratio value between 1-5 indicating that the Si and Al source in the reaction were the albite and clinoptilolite because quartz is inert at low pressure and temperature considered here.

The XRD diffractograms obtained from each experiment were classified in four groups showed in the Figure 2 and four samples were classified separately. The separately depicted experiment are 13, 18, 19 and 31 (Figure 3a-d). Moreover, the relative intensity in the XRD diffractograms was calculated to evaluate the presence of original aluminosilicates and the zeolite P. It is important to note that the amorphous halo was identified in all of the diffractograms.

Figure 2a shows the XRD diffractograms and the relative presence of albite, clinoptilolite, quartz and zeolite P in the experimental prepared samples. The intensity of the peak at  $22.5\ 2\theta$  that corresponds to clinoptilolite in the original sample is lower than the experiments related at the group 1. Zeolite P has a relative intensity average of  $20.47 \pm 1.16$  arbitrary units (au) indicating that the source of Si and Al was the clinoptilolite because the intensity of albite remains constant: the albite originally has a relative intensity of 28.22 au while the average in the experiments of group 1 is  $21.99 \pm 1.19$  au. The presence of amorphous halo is different in each diffractogram.

Table 6. Experimental matrix and results of synthesis of zeolitic material from natural clinoptilolite.

Exp.	Experimental factor					Results		
	CTAB, g/mL	Time, h	Temp., ° C	NaOH, M	Sol/liq., g/mL	Identified phases	Surface area, m <sup>2</sup> /g	Adsorption capacity of CO <sub>2</sub> , mmol/g
1	0.015	24	60	2	0.1	A, C, P, Q	36.85	2.3
2	0.03	24	90	4	0.1	P	27.66	1.8
3	0.015	48	60	4	0.1	P	34.27	2.2
4	0.03	48	90	2	0.1	C, P, Q	40.73	2
5	0.03	24	60	2	0.1	A, C, P, Q	40.44	2.2
6	0.03	24	90	2	0.2	A, C, P, Q	27.36	2.2
7	0.015	48	90	4	0.1	P	31.61	1.8
8	0.015	48	60	4	0.2	P	26.89	1.6
9	0.03	24	60	4	0.1	A, C, P, Q	45.47	1.5
10	0.015	24	60	4	0.1	P	25.24	1.5
11	0.015	48	90	2	0.1	C, P, Q	31.56	1.8
12	0.015	24	90	4	0.2	P	21.21	1.5
13	0.03	48	60	2	0.1	C, P	35.24	1.8
14	0.03	24	90	4	0.2	P	27.6	1.6
15	0.03	24	60	2	0.2	A, C, P, Q	31.63	2
16	0.03	48	90	4	0.1	P	40.82	1.7
17	0.03	48	60	2	0.2	A, C, P, Q	30.85	2.4
18	0.03	48	90	4	0.2	C, P	28.71	1.4
19	0.03	24	60	4	0.2	A, C, P	28.71	1.9
20	0.03	24	90	2	0.1	C, P, Q	32.68	2
21	0.015	48	60	2	0.1	C, P, Q	28.25	1.9
22	0.03	48	60	4	0.2	P	23.6	1.4
23	0.015	48	60	2	0.2	A, C, P, Q	28.83	2
24	0.015	24	90	4	0.1	P	26.4	1.7
25	0.015	24	60	2	0.2	A, C, P, Q	25.65	2.5
26	0.015	48	90	2	0.2	A, C, P, Q	26.37	2.6
27	0.015	24	60	4	0.2	A, C, P, Q	38.65	2.5
28	0.015	24	90	2	0.2	A, C, P, Q	30.2	2
29	0.015	48	90	4	0.2	P	26.87	1.4
30	0.03	48	60	4	0.1	P	32.48	1.6
31	0.015	24	90	2	0.1	C, P, Q	30.37	2.8
32	0.03	48	90	2	0.2	A, C, P, Q	29.77	1.7
			Natural clinoptilolite			C, Q, A	19.563	1.4

In the group 2 (Figure 2b) is notable the presence of zeolite P and the amorphous halo that is superposed over the peaks of the original minerals in the sample of clinoptilolite. Two principal peaks are observed together; for example, the peaks at 12.49 and 13.41 2θ that indicates the coexistence of zeolite type P tetragonal and cubic. Katović *et al.*, (1989) studied the formation of zeolites type P establishing that the formation of zeolite type P tetragonal crystallized in first time and the cubic in the second one. These authors explained that the formation of zeolite type P cubic occurs by the dissolution of the tetragonal specie observing a major consume of Al presents

in the gel of synthesis. In the present study the clinoptilolite and albite were source of Si and Al for the synthesis of the two species of zeolite type P. The signals of quartz are not observed but that is not the evidence of its dissolution because the presence the amorphous halo is observed. As similar in the group 1 this group should have an amorphous material. The experiment belong to this group were obtained with the high concentration of NaOH studied indicating the possibility for using an intermediate concentration. However, the others experimental factors have to be considering to achieve a complete analysis.

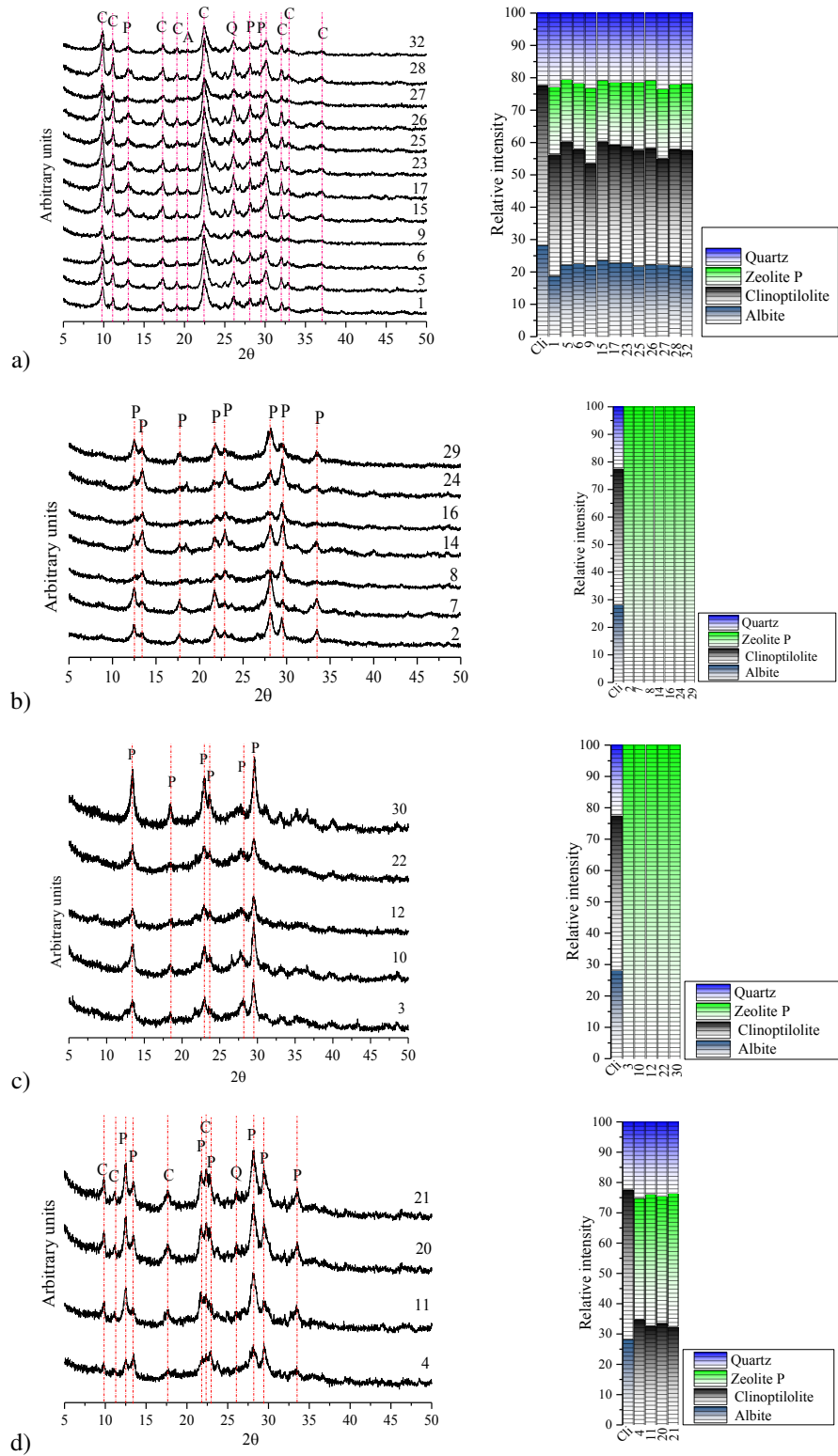


Fig. 2. Diffractograms of experiments a) group 1 (1, 5, 6, 9, 15, 17, 23, 25, 26, 27, 28 and 32); b) group 2 (4, 11, 20 and 21); c) group 3 (3, 10, 12, 22 and 30); d) group 4 (4, 11, 20 and 21).

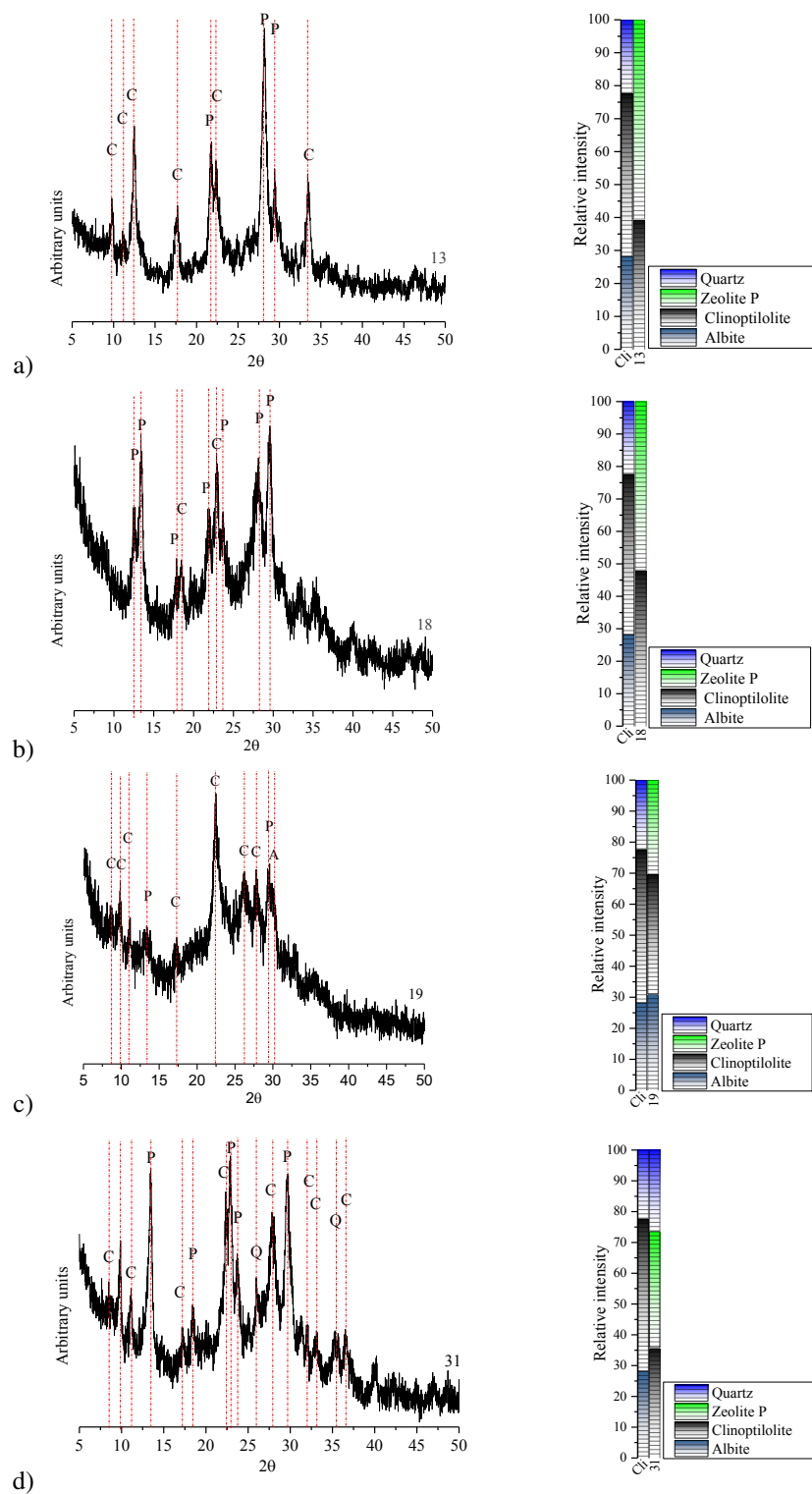


Fig. 3. Diffractograms of experiments a) 13, b) 18, c) 19 and d) 31.

For the group 3, the two peaks of the species of zeolite type P are not identified. Only the peak that correspond at zeolite type P tetragonal are observed. In the same form by group 2 the experiments of the group 3 were obtained with the high concentration. In Figure 2c are showed peaks with different amplitude. For example, the sample 22 has a wide peak in comparison with the sample 30. The unique difference in the preparation method was the solid/liquid ratio: for the experiment 22 was of 0.2 g/mL while experiment 30 was 0.1 g/mL. The last one indicates that a major amount of clinoptilolite in the sample promotes the slow growth of the crystal of the zeolite P. It is the same case for the experiments 10 and 12. The first one has a higher intensity than the experiment 12 because the experiment 10 was achieved with a low solid/liquid ratio that promotes a rapid growth of crystals of zeolite P. Figure 2d shows the diffractograms of the group 4 which were identified clinoptilolite, zeolite P and quartz. For albite, the principal peaks not appeared indicating the possible dissolution of this mineral. Moreover, the presence of zeolite type P tetragonal and cubic are observed. Between the experiments 11 and 21 the only differences in the method of preparation was the temperature, 90 and 60° C, respectively. In the diffractogram of the experiment 21 the peaks of zeolite type P tetragonal and cubic are more intense than in the case of experiment 11. In the last one the peaks that correspond at zeolite P tetragonal are lower than the zeolite P cubic indicating that the dissolution of zeolite P tetragonal to form the cubic structure. It is in accord with the study of Katović *et al.*, (1989) which the sequence of formation is as follow: amorphous material→zeolite P tetragonal→zeolite P cubic. The experiments 13, 18, 19 and 31 were not classified because the difference in the form and position of the observed peaks. In the Figure 3a is depicted the diffractogram of experiment 13 which the peaks of zeolite P cubic are more intense than the tetragonal one. In comparison with the experiment 13, the 18 presents a most intense of the peaks of zeolite P tetragonal, that is, the correlation to explain the formation of zeolite P species is difficult to observed. Under this consideration the results of intensities in the diffractograms were statistically analyzed in order to obtain a correlation between the abundance of mineralogical phases and the surface area.

### 3.3 Statistical analysis of the mineralogical phases identified

Principal effects and interaction of effects were analyzed for each phase identified considering them as a response. The normal probability plots are depicted in Figure 4.

Figure 4 shows the significance effects on the response. The experimental factors with non-significance effect for the response are according the straight line but the factors without significant effect are depicted in other position. For the case of the dissolution of albite showed in the Figure 4a the significant effect is the solid/liquid ratio and the NaOH concentration. For the clinoptilolite and quartz dissolution the NaOH concentration is the principal effect. In the case of the occurrence of zeolite P the NaOH was also the principal effect. To determine the negative or positive effect by the experimental factors the Pareto charts were depicted (Figure 5).

In Figure 5a-c the NaOH concentration appear with a negative effect, that is, the increase of NaOH concentration decrease the intensity of albite, clinoptilolite and quartz in the reaction of preparation. On the other hand, the Si and Al present in the albite and clinoptilolite are available in the gel of synthesis to form the zeolite P, that is, to increase the intensity of the signal for this zeolite the high amount of NaOH in the reaction is necessary. CTAB have not a principal effect in all of the cases. CTAB template has the effect to form the small structures by the formation of micelles at the evaluated conditions here. Several studies show that the crystal size is affected by the presence of CTAB in the reaction of formation of zeolites (Katović *et al.*, 1989; Kong *et al.*, 2009; Wang *et al.*, 2012). In this case, the crystal size of zeolite P synthesized by natural clinoptilolite here was affected by the CTAB; however, the impurities in the synthesis, as quartz principally, and the dissolution of albite and the clinoptilolite were determinant factors to inhibit this effect. That is, the formation of micelles of CTAB were not successfully achieved. However, the results of CO<sub>2</sub> adsorption capacity is satisfactory because the high values; for example, values higher than 2 mmol/g were founded. The analysis of the Table 1 and 2 showed that the average value for CO<sub>2</sub> adsorption capacity of zeolites is 2.35 mmol/g being the 4 the maximum value. For the case of mesoporous materials (Table 2), the maximum value is 4 mmol/g. The zeolitic material synthesized in the present study have a minimum, maximum and average value of 1.4, 2.8 and 1.92 mmol/g, respectively.



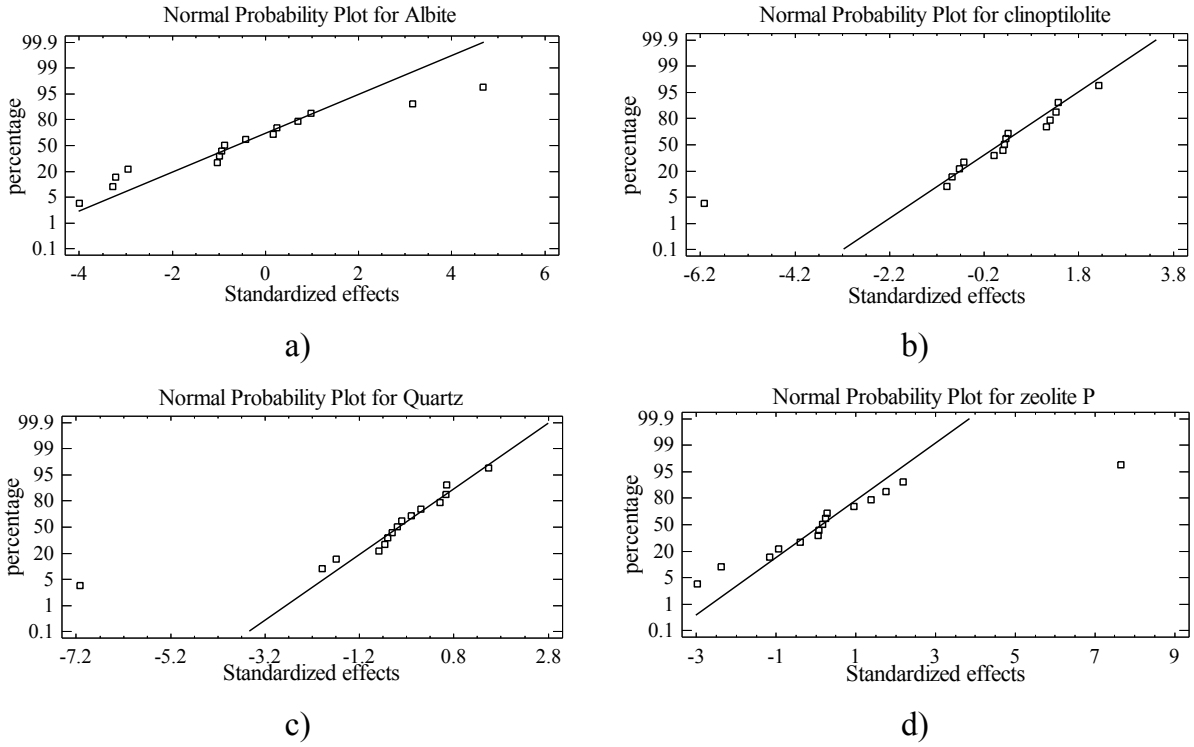


Fig. 4. Normal probability for the a) albite, b) clinoptilolite, c) quartz and d) zeolite P.

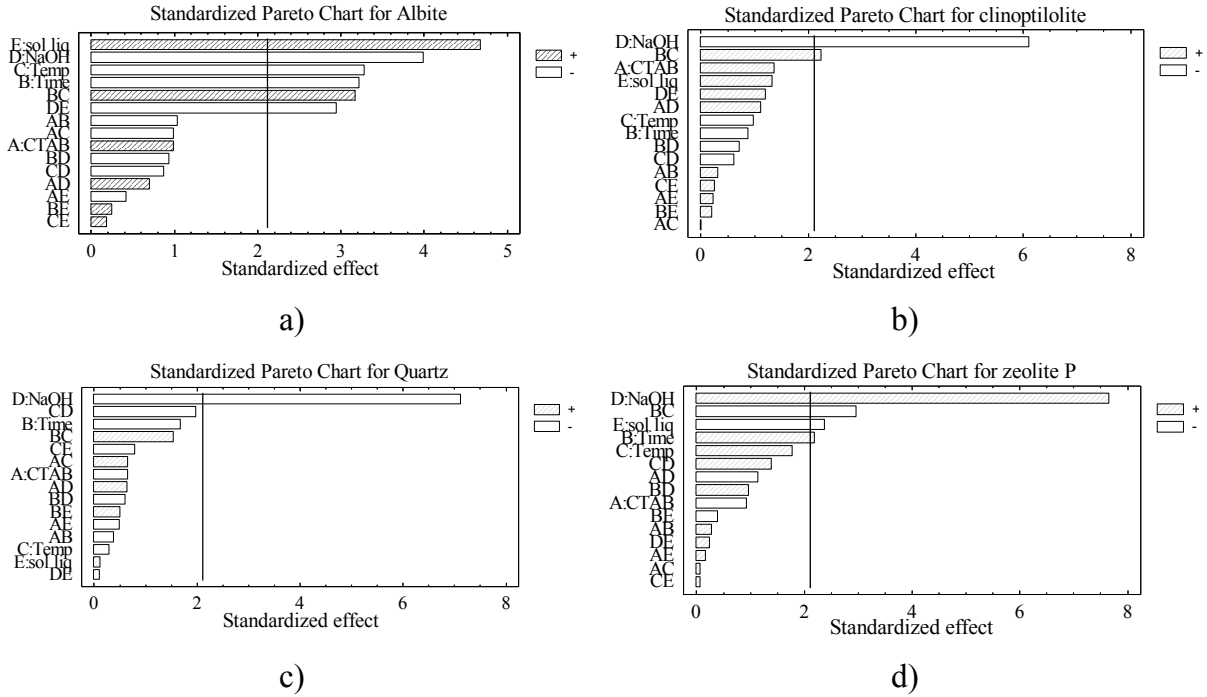


Fig. 5. Pareto diagram for the a) albite, b) clinoptilolite, c) quartz and d) zeolite P.

These values, although correspond to zeolitic material impregnated with DEA are significances.

The results of adsorption capacity of CO<sub>2</sub> showed in the Table 2 were not analyzed under the statistical methodology due to DEA impregnation was not considered as a principal factor in the experimental methodology. However, it is important to note that the presence of the DEA in the synthesized zeolites here improved the CO<sub>2</sub> adsorption.

### 3.4 Statistical analysis of surface area and CO<sub>2</sub> adsorption capacity of zeolitic material

Surface area is an important parameter to establish the adsorption capacity in the materials. It is convenient to have high values of surface area in the case of zeolitic materials. This parameter indicates the presence of porosity in the range of micro or mesoporous, principally. The Figure 6 shows the effects with significance effect to surface area of the synthesized zeolitic materials. The parameters with significance effect were the solid/liquid ratio and time:temperature of reaction interaction; the values of the surface area obtained are slightly low in relation with the synthetic zeolites obtained with pure reactants.

There was only one factor considered with significance over the surface area and the CO<sub>2</sub> adsorption capacity. For this reason, the analysis was not achieved. This indicates the low correlation between the surface area and CO<sub>2</sub> adsorption capacity and the considered factors.

The values of surface area are similar to reported by other works; for example, Derkowski *et al.*, (2006) determinate that the zeolite P synthesized has a surface area of 39 m<sup>2</sup>/g. Tang *et al.*, (2015) determined a surface area of 42.08 m<sup>2</sup>/g for zeolite P. In this work the means value of surface area was 30.2±5.8 m<sup>2</sup>/g with a high and low value of 45.58 and 21.37, respectively.

For the case of CO<sub>2</sub> adsorption capacity the mean value is 1.92±0.38 mmol/g with a high and low value of 2.8 and 1.4, respectively. These values are higher than in the case of natural clinoptilolite. For this zeolite the CO<sub>2</sub> adsorption capacity was 1.4 mmol/g that is low in relation with the zeolitic material synthesized here. In other hand Wdowin *et al.*, (2012) reported a sorption capacity of CO<sub>2</sub> of zeolite P of 0.39 mmol/g.

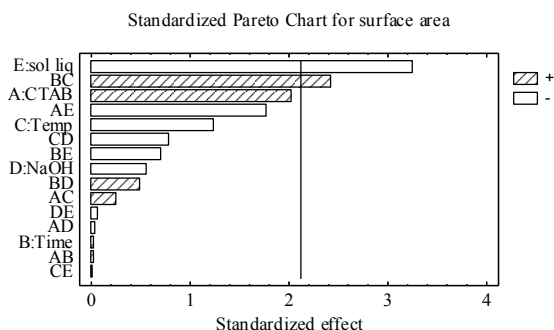


Fig. 6. Pareto diagram for the surface area of the synthesized zeolitic material.

## Conclusions

In this study the preparation of zeolite P from a clinoptilolite natural was achieved. The natural clinoptilolite contained quartz and albite, as principal impurities, and affected the synthesis of formation of zeolite P. Clinoptilolite and albite were the principal sources of Si and Al and the NaOH concentration affected the dissolution of these minerals. For the case of quartz, there is not a significance factor in the synthesis process. The zeolite P synthesized, under DEA impregnation, was used to capture CO<sub>2</sub>. The maximum value was 2.8 mmol/g that represents a high value respect to other investigations. The process could achieve a major scale and produce zeolites with high CO<sub>2</sub> adsorption capacity.

## Acknowledgements

Adriana Sánchez-Ruíz acknowledges the Master grant on behalf of CONACYT. Authors thank to SENER-CONACYT for the financial support (Grant 247006) and Leticia García Montes de Oca from-IINGEN-UNAM for her assistance in the textural analysis.

## References

- Araki, S., Kiyohara, Y.m Tanaka, S.m Miyake, Y. (2012). Adsorption of carbon dioxide and nitrogen on zeolite rho prepared by hydrothermal synthesis using 18-crown-6 ether. *Journal of Colloid Interface Science* 388, 285-190.

- Beck, J.S., Vartuli, J.C., Roth, W.J., Leonowicz, M.E., Schmitt, K.D. Chu, C.T-W., Olson, D.H., Sheppard, E.W., McCulle, S.B., Higgins, J.B., Schlenker, J.L. (1992). A new family of mesoporous molecular sieves prepared with liquid crystals templates. *Journal of the American Chemical Society* 114, 10834-10843.
- Behin, J., Kazemian, H., Rohani, S. (2016). Synthesis and characterization of mesoporous molecular sieve MCM-41 prepared from natural clinoptilolite zeolite. Sonochemical synthesis of zeolite NaP from clinoptilolite. *Ultrasonics Sonochemistry* 28, 400-408.
- Brundu, A., Cerri, G. (2015). Thermal transformation of Cs-clinoptilolite to CsAlSi<sub>5</sub>O<sub>12</sub>. *Microporous and Mesoporous Materials* 208, 44-49.
- Cheung, O., Bacsik, Z., liu, Q., Mace, A.m Hedin, N.(2013). Adsorption kinetics for CO<sub>2</sub> on highly selective zeolites NaKA and nano-NaKA. *Applied Energy* 112, 1326-1336.
- de Fazio, A., Brotzu, P. Ghiara, M.R., Fercia, M.L., Lonis, R., Sau, A. (2008). Hydrothermal treatment at low temperatura of Sardinian clinoptilolite-bearing ignimbrites for increasing cation exchange capacity. *Periodico di Mineralogia* 77, 79-91.
- Derkowski, A., Franus, W., Beran, E., Csímerová, A. (2006). Properties and potential applications of zeolitic materials produced from fly ash using simple method of synthesis. *Powder Technology* 166, 47 - 54.
- Espejel-Ayala, F., Solís-López, M., Schouwenaars, R., Ramírez-Zamora, R.M. (2015). Synthesis of zeolite P ussing copper mining tailings. *Revista Mexicana de Ingeniería Química* 14, 205-212.
- Hefti, M., Marx, D., Joss, L., Mazzotti, M. (2015). Adsorption equilibrium of binary mixtures of carbon dioxide and nitrogen on zeolites ZSM-5 and 13X. *Microporous and Mesoporous Materials* 215, 215-228.
- Hernández-Huesca, R., Aguilar-Armenta, G. (2002). Calores isostéricos de adsorción de CO<sub>2</sub> en zeolitas naturales mexicanas. *Revista de la Sociedad Química de México* 46, 109-114.
- Heydari-Gorji, A., Belmabkhout, Y., Sayari, A. (2011). Polyethylenimine-impregnated mesoporous silica: effect of amine loading and surface alkyl chains on CO<sub>2</sub> adsorption. *Langmuir* 27, 12411-12416.
- Hosseini, B., Nourbakhsh, A.A., MacKenzie, K.J.D. (2015). Magnesiothermal synthesis of nanostructured SiC from natural zeolite (clinoptilolite) and mesoporous carbon CMK-1. *Ceramics International* 41, 8809-8813.
- Jiang, Q., Rentschler, J., Sethia, G., Weinman, S., Perrone, R., Liu, K. (2013). Synthesis of T-type zeolite nanoparticles for the separation of CO<sub>2</sub>/N<sub>2</sub> and CO<sub>2</sub>/CH<sub>4</sub> by adsorption process. *Chemical Engineering Journal* 230, 380-388.
- Jing, Y., Wei, L., Wang, Y., Yu, Y. (2014). Synthesis, characterization and CO<sub>2</sub> of mesoporous SBA-15 adsorbents functionalized with melamine-based and acrylate-based amines dendrimers. *Microporous and Mesoporous Materials* 183, 124-133.
- Joshi, M.S., Joshi, V.V. (1985). Hydrothermal transformation of clinoptilolite. *Bulletin of Materials Science* 7, 475-481.
- Kacem, M., Pellerano, M.m Delebarre, A. (2015). Pressure swing adsorption for CO<sub>2</sub>/N<sub>2</sub> and CO<sub>2</sub>/CH<sub>4</sub> separation: comparison between activated carbons and zeolites. *Fuel Processing Technology* 138, 271-283.
- Kamali, M., Vaezifar, S., Kolahduzan, H., Malekpour, A., Abdi, M.R. (2009). Synthesis of nanozeolite A from natural clinoptilolite and aluminum sulfate; optimization of the method. *Powder Technology* 189, 52-56.
- Kang, Sh-J., Egashira, K., Yoshida, A. (1998). Transformation of a low-grade Korean natural zeolite to high cation exchanger by hydrothermal reaction with or without fusion with sodium hydroxide. *Applied Clay Science* 13, 117-135.
- Katović, A., Subotić, B., Smit, I., Despotović, L.A. (1989). Crystallization of tetragonal (B8) and cubic (B1) modifications of zeolite NaP from freshly prepared gel. Part 1. *Zeolites* 9, 45-53.
- Kazemian, H., Modarress, H., Kazemi, M., Farhadi, F. (2009). Synthesis of submicron zeolite LTA particles from natural clinoptilolite and industrial grade chemicals using one stage procedure. *Powder Technology* 196, 22-25.

- Klinton, W., Huang, Ch-H., Tan, Ch-S. (2014). Polyallylamine and NaOH as a novel binder to pelletize amine-functionalized mesoporous silicas for CO<sub>2</sub> capture. *Microporous and Mesoporous Materials* 197, 278-287.
- Lee, Ch.H., Hyeon, D.H., Jung, H., Chung, W., Jo, D.H., Shin, D.K., Kim, S.H. (2015). Effect of pore structure and Pei impregnation on carbon dioxide adsorption by ZSM-5 zeolites. *Journal of Industrial Engineering Chemistry* 23, 251-256.
- Lin, L-Y., Bai, H. (2012). Aerosol processing of low-cost mesoporous silica spherical particles from photonic industrial waste powder for CO<sub>2</sub> capture. *Chemical Engineering Journal* 197, 215-222.
- Liu, L., Du, T., Li, G., Yang, F., Che, Sh. (2014). Using one waste to tackle another: preparation of a CO<sub>2</sub> capture material zeolite from laterite residue and bauxite. *Journal of Hazardous Materials* 278, 551-558.
- Pérez-Escobedo, A., Díaz-Flores, P.E., Rangel-Méndez, J.R., Cerino-Cordova, F.J., Ovando-Medina, V.M., Alcalá-Jáuregui, J.A. (2016). Fluoride adsorption capacity of composites based on chitosan-zeolite-algae. *Revista Mexicana de Ingeniería Química* 15, 139-147.
- Ridha, F.N., Webley, P.A. (2009). Investigation of the possibility of low pressure encapsulated of carbon dioxide in potassium chabazite (KCHA) and sodium chabazite (NaCHA) zeolites. *Journal of Colloid Interface Science* 337, 332-337.
- San, O., Abali, S., Hosten. C. (2003). Fabrication of microporous ceramics from ceramic powders of quartz-natural zeolite mixtures. *Ceramics International* 29, 927-931.
- Sanz, R., Calleja, G., Arencibia, A. Sans-Pérez, E.S. (2015). CO<sub>2</sub> capture with pore-expanded MCM-41 silica modified with amino groups by double functionalization. *Microporous and Mesoporous Materials* 209, 165-171.
- Serna-Guerrero, R., Sayari, A. (2010). Modeling adsorption of CO<sub>2</sub> on amine-functionalized mesoporous silica. 2: kinetics and breakthrough curves. *Chemical Engineering Journal* 161, 182-190.
- Shindo, T., Nagai, Y., Ikeuchi, T., Ozawa, S. (2010). Synthesis of MCM-41 with zeolite P from natural clinoptilolite for silica-alumina source under hydrothermal conditions in alkaline media. *International Journal of the Society Materials Engineering for Resources* 18, 1-6.
- Shindo, T., Narita, Ch., Ozawa, S. (2008). Synthesis and characterization of mesoporous molecular sieve MCM-41 prepared from natural clinoptilolite zeolite. *International Journal of the Society Materials Engineering for Resources* 15, 46-49.
- Steenefeldt, R., Berger, B., Torp, T.A. (2006). CO<sub>2</sub> capture and storage closing the knowing-doing gap. *Chemical Engineering Research and Design* 84, 739-763.
- Tang, Q., Ge, Y.; Wang, K., He, Y., Cui, X. (2015). Preparation of porous P-type zeolites spheres with suspension solidification method. *Materials Letters*, 558-560.
- Tunc, T., Demirkiran, S. (2014). The effects of mechanical activation on the sintering and microstructural properties of cordierite produced from natural zeolite. *Powder Technology* 260, 7-14.
- Wang, Y., Lin, F. J (2009). Synthesis of high capacity cation exchangers from a low-grade Chinese natural zeolite. *Journal of Hazardous Materials* 166, 1014-1019.
- Wdowin, M., Franus, W., Panek, R. (2012). Preliminary results of usage possibilities of carbonate and zeolitic sorbents in CO<sub>2</sub> capture. *Fresenius Environmental Bulletin* 21, 3726-3734.
- Wong-Ng., Kaduk, J.A., Huang, Q., Espinal, L., Li, L., Burrell, J.W. (2013). Investigation of NaY zeolite with adsorbed CO<sub>2</sub> by neutron powder diffraction. *Microporous and Mesoporous Materials* 172, 95-104.
- Yang, F-M., Chen, L., Au, Ch-T., Yin, Sh-F. (2015). Preparation of triethylenetetramine-modified zirconosilicate molecular sieve for carbon dioxide adsorption. *Environmental Progress and Sustainable Energy* 34, 1814- 1821.
- Yang, H., Xu, Z., Fan, M., Gupta, R., Slimane R.B., Bland, A.E., Wright, I. (2008). Progress in

carbon dioxide separation and capture: a review. *Journal of Environmental Science* 20, 14-27.

Yoleva, A., Djambazov, S., Chernev, G. (2011). Influence of the pozzolanic additives trass

and zeolite on cement properties. *Journal of the University of Chemical Technology and Metallurgy* 46, 261-266.